Journal of Crystal Growth 418 (2015) 32–37

Contents lists available at ScienceDirect

Journal of Crystal Growth

journal homepage: www.elsevier.com/locate/jcrysgro

Nonstoichiometric composition shift in physical vapor deposition of CdTe thin films

Ken K. Chin [a,b], Zimeng Cheng [a,b,*], Alan E. Delahoy [a,b]

[a] Department of Physics, New Jersey Institute of Technology, University Heights, Newark, NJ 07102, USA
[b] CNBM New Energy Materials Research Center, New Jersey Institute of Technology, University Heights, Newark, NJ 07102, USA

ARTICLE INFO

Article history:
Received 2 April 2014
Received in revised form
7 January 2015
Accepted 5 February 2015
Communicated by R.M. Biefeld
Available online 14 February 2015

Keywords:
A1. Growth models
A3. Physical vapor deposition processes
B1. Cadmium compounds
B2. Semiconducting II–VI materials

ABSTRACT

While it is being debated whether Cd vacancy is an effective p-dopant in CdTe, and whether CdTe thin film in solar energy application should be Cd-deficient or Cd-rich, in the theory of CdTe physical vapor deposition (PVD) it has been assumed that both the source material and the thin film product is stoichiometric. To remediate the lack of effective theory, a new PVD model for CdTe photovoltaic (PV) modules is presented in this work, in which the composition of the CdTe thin film under growth is a parameter determined by the source CdTe composition as well as the growth condition. The solid phase $Cd_{1-\delta}Te_{1+\delta}$ compound under deposition temperature is treated as a solid solution with *a* mole of excess pure Te or Cd as solute and one mole of congruently grown CdTe as solvent. Assuming that the vapor pressure of Te_2 can be calculated by using the law of solid solution $P_{Te}=H_0+aH_1+a^2H_2$ round the congruent composition, where the molar number *a* and the constants H_0, H_1 and H_2 as functions of temperature *T* are extracted from the experimental data. Thus, the mole fraction of solute in the grown CdTe thin film as well as the growth rate, as a function of the solute mole fraction in the source CdTe can be determined.

1. Introduction

Physical vapor deposition (PVD) of CdTe thin film is widely used in photovoltaic (PV) module production. So far in the close-spaced sublimation (CSS) PVD modeling of CdTe as well as other semiconductor compounds, it is assumed that both the source material and the thin film product are stoichiometric [1,2]. The diffusion-limited growth model of CSS was discussed by Bube et.al. [1] in detail, where the ratio of the fluxes of Cd atoms and Te_2 molecules from the source to the substrate were assumed to be 2:1 in order to get stoichiometric CdTe films. This assumption is accurate enough for the calculations of the growth rate. It is well known, however, that the minor deviation of the composition of thin film CdTe from its perfect stoichiometric crystal has major effect on its electronic properties [3]. A question arises: Is it possible to find the proper temperatures and background pressure, as well as a source material—for example the Cd-deficient (or Te-rich)—with the proper ratio of Cd/Te so that the grown CdTe thin film product has the optimized Cd/Te ratio and electronic properties?

From the fitted PTX curves by Greenberg [4], the partial pressure curves of Cd and Te_2 as a function of non-stoichiometry under each temperature cross each other at a particular composition, very close to the congruent sublimation point. The cross point of the two partial pressure curves is always at Te rich side, making CdTe films grown by CSS always Cd-deficient (or Te-rich). The CdTe compound (denoted as $Cd_{1-\delta}Te_{1+\delta}$) were considered as a function of atomic percentage of Te in the PTX works of Greenberg, where the atomic fraction number of Te F_{Te} is linked to *x* as $F_{Te}=(1+\delta)/2$. The solid CdTe compound can be treated as a solid solution with either stoichiometric CdTe as solvent and excess pure Te atoms as solute, or congruently-grown CdTe (Te rich) as solvent and excess Cd or Te as solute. The molar number *a* is defined as the mole concentration of the solute in one mole solvent. Assuming that the partial vapor pressures obey the law of solid solution $P_{(Cd\ or\ Te)}=H_0+aH_1+a^2H_2$, where the molar number *a* of the solvent and the constants H_0, H_1 and H_2 as functions of temperature *T* can be extracted from the experimental data and will be discussed below. Therefore, the answer to the question seems to be positive.

2. Results and discussion

This part is organized around three different sections. First, a thermodynamic model is introduced to discuss how excess Cd and Te is treated as the solute in a solvent comprised of vapor phase stoichiometric, solid phase stoichiometric and congruent PVD conditions. Next, we consider congruent PVD condition as the

---

* Corresponding author. Tel.: +1 3479786646.
E-mail addresses: zc6@njit.edu, ben.cheng2009@gmail.com (Z. Cheng).

http://dx.doi.org/10.1016/j.jcrysgro.2015.02.018

solvent and refine this model using PTX partial pressure data published by Greenburg [4]. Lastly, we use this model to calculate the resulting composition of films deposited by close-spaced sublimation, by assuming different source material stoichiometry.

2.1. Nonstoichiometric compound solid solution model

According to the classic Henry's law, the saturated vapor pressure of solute B in a solution is

$$P_B = \gamma_B X_B P_B^o = H_1 X_B \tag{1}$$

where X_B is the molar number of the solute B, P_B^o the saturated vapor pressure of pure B, and γ_B the activity coefficient of solute B dissolved or dispersed in solvent A. If the attraction among solute atoms is greater than that between the solute atom B and the solvent atom A, γ_B is less than 1. Otherwise, γ_B is greater than 1. Combining P_B^o and γ_B, we have H_1, which is independent of X_B. For solution with very low solute concentration, $X_B \ll 1$, we have a constant linearity coefficient H_1, as shown in Eq. (1). To simplify discussion, we start with an A-deficient or B-rich compound semiconductor AB, the cation element A and the anion element B being volatile. There are three special points, as shown in Fig. 1, in the diagram of saturated vapor pressures of A and B under solid–vapor equilibrium condition at an elevated temperature *T*.

(1) Point *V*—vapor phase stoichiometric
$P_A = P_B$, or molar number $X_A = X_B$ in vapor phase, but nonstoichiometric in solid phase as shown by its composition $A_{1-\delta_V}B_{1+\delta_V}$

$$\begin{cases} A_{1-\delta_V}B_{1+\delta_V} = (1-\delta_V)A + (1+\delta_V)B - \Delta G_V \\ \text{with} \quad P_{A,V} = P_{B,V} \quad \text{satisfying} P_{A,V}^{1-\delta_V} P_{B,V}^{1+\delta_V} = P_{A,V}P_{B,V} = \exp\left(-\frac{\Delta G_V}{RT}\right) \end{cases} \tag{2}$$

(2) Point *S*—solid phase stoichiometric
Stoichiometric AB or $X_A = X_B$ in solid phase, but nonstoichiometric in vapor phase with $P_A > P_B$; or $X_A > X_B$;

$$\begin{cases} AB = A + B - \Delta G \\ \text{with} \quad P_{A,S} > P_{B,S} \quad \text{satisfying} \quad P_{A,S}P_{B,S} = \exp\left(-\frac{\Delta G_S}{RT}\right) \end{cases} \tag{3}$$

(3) Point *C*—congruent PVD condition, with same molar composition in solid as well as vapor phase, *C* being at right and very close to *V*

$$\begin{cases} A_{1-\delta_C}B_{1+\delta_C} = (1-\delta_C)A + (1+\delta_C)B - \Delta G_C \\ \text{with} \quad \frac{P_{A,C}}{P_{B,C}} = \frac{1-\delta_C}{1+\delta_C} \quad \text{satisfying} \quad P_{A,C}^{1-\delta_C} P_{B,C}^{1+\delta_C} = \exp\left(-\frac{\Delta G_C}{RT}\right) \end{cases} \tag{4}$$

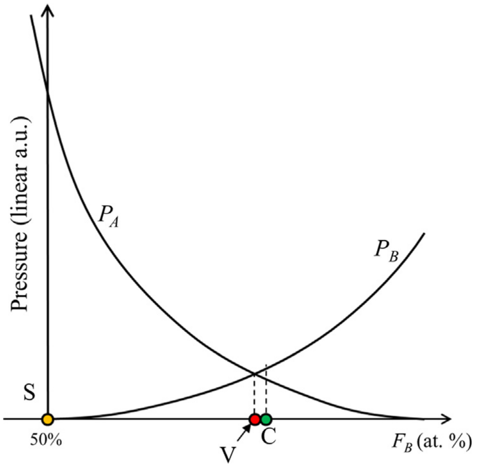

Fig. 1. Partial pressures of saturated pressures of A and B of different solid composition under solid–vapor equilibrium condition at an elevated temperature *T*. Three special points *V*, *S* and *C* are indicated.

The PVD source material as well as the desired nonstoichiometric compound thin film product $A_{1-a}B_{1+a}$ is, however, not of the composition *V*, *S* or *C*. Although much smaller than 1, *a* may be much greater than $\delta_V$or δ_C. For a A-deficient or B-rich compound, we hypothesize that $A_{1-\delta}B_{1+\delta}$ may behave as a solid solution with solute B "dissolved" in the solvent AB, or a solid solution with excess A or B "dissolved" in the solvent $A_{1-\delta_V}B_{1+\delta_V}$ or $A_{1-\delta_C}B_{1+\delta_C}$. As a phenomenological hypothesis, which is based on empirical data, the solid solution may have all 3 forms of the compound as solvents. The 3 cases in the B-rich compound are (in the format of normalized solvent+molar number $a \times$ solute):

$$A_{1-\delta}B_{1+\delta} \Rightarrow AB + \frac{2\delta}{1-\delta}B \tag{5}$$

$$A_{1-\delta}B_{1+\delta} \Rightarrow \begin{cases} A_{1-\delta_V}B_{1+\delta_V} + \frac{2(\delta-\delta_V)}{1-\delta}B & (\text{if } \delta > \delta_V) \\ A_{1-\delta_V}B_{1+\delta_V} + \frac{2(\delta_V-\delta)}{1+\delta}A & (\text{if } \delta < \delta_V) \end{cases} \tag{6}$$

$$A_{1-\delta}B_{1+\delta} \Rightarrow \begin{cases} A_{1-\delta_C}B_{1+\delta_C} + \frac{2(\delta-\delta_C)}{1-\delta}B & (\text{if } \delta > \delta_C) \\ A_{1-\delta_C}B_{1+\delta_C} + \frac{2(\delta_C-\delta)}{1+\delta}A & (\text{if } \delta < \delta_C) \end{cases} \tag{7}$$

Independent of the selection of solvent, the solid solution satisfies the solid–vapor equilibrium condition of chemical reaction. Since δ_V,$\delta_C$and *a* are all $\ll 1$ and $\Delta G \approx \Delta G_V \approx \Delta G_S \approx \Delta G_C$, the solid–vapor equilibrium condition of compounds *S*, *V*, *C* as well as solid solution can all be expressed as the equation of stoichiometric reaction of solid phase compound and vapor phase components

$$P_A P_B = K = \exp\left(-\frac{\Delta G}{RT}\right) \tag{8}$$

In addition, the solid solution must satisfy the law of solute vapor pressure P_B

$$P_B = H_o + aH_1 + a^2 H_2 \tag{9}$$

where the molar number *a* is expressed in Eqs. (5)–(7) with different solvents (the molar number *a* equals to the factor in front of the solute). Note that the classical Henry's law of solution Eq. (1) does not have the constant term H_0, since P_B=0 when there is no solute. On the contrary, for AB of volatile component A and B, when solute concentration=0, the solvent still exerts a pressure P_B. Another difference—of choice, not necessity—from Eq. (1) is: Eq. (9) has a second order term following the Taylor expansion to show the trend of solute pressure P_B as its molar number *a* increases.

2.2. Refinement of the model with experimental data

Experimentally, it is very difficult to obtain an accurate reading of partial pressure when the other partial pressure is dominant in the vapor phase. In this case, it is necessary to measure the dominant partial pressure component and then force the confinement in Eq. (8) to get the other partial pressure component. Most CdTe phase diagrams and vapor pressure data are measured at much higher temperature than the sublimation temperature. Using available high temperature data, we can estimate the growth behavior at adjacent lower temperatures. The best-fitted equilibrium partial pressure curves of Cd and Te_2 under four different temperatures as a function of F_{Te} are shown in Fig. 2

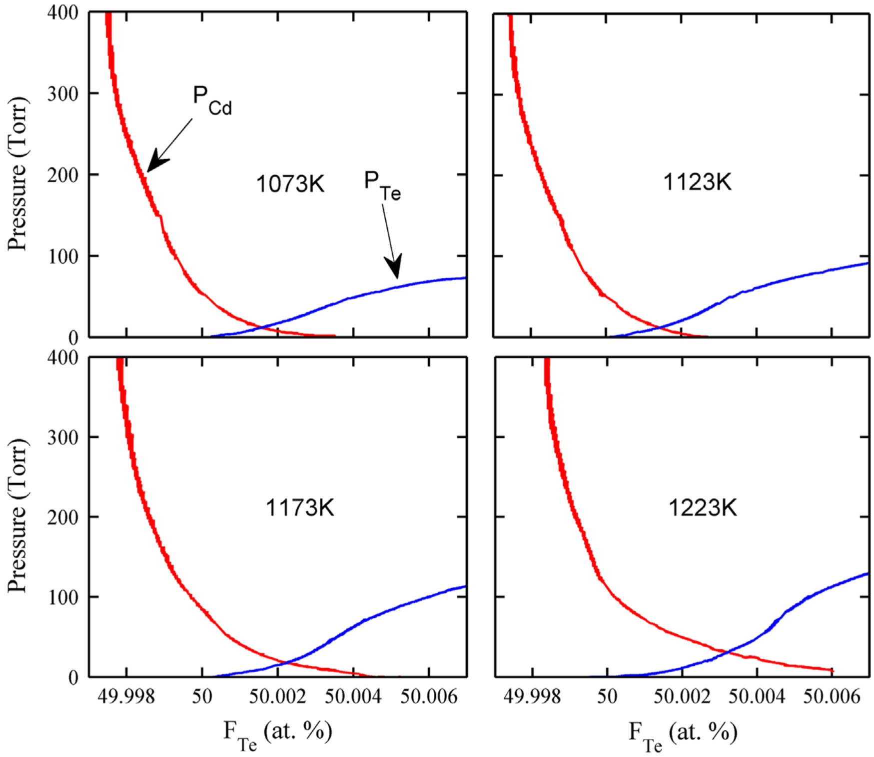

Fig. 2. The best-fitted equilibrium partial pressure curves of Cd and Te_2 under four different temperatures as a function of F_{Te}.

[4]. It is clear that under thermodynamic equilibrium, the solid phase composition (shown by Te atomic fraction number F_{Te}) is very different from that of the vapor phase $[2P_{Te2}/(P_{Cd}+2P_{Te2})]$. According to the experimental data at 1073 K, the vapor's composition will become almost Te free when $F_{Te} < 49.996\%$ in the source solid, and will become almost Cd free when $F_{Te} > 50.008\%$ in the source solid, although there is still nearly 50% Te in the solid. The law of solute vapor pressure is applicable because the molar number a of solute $\lessdot 1$ in such solid composition range.

This behavior is similar regardless whether the solid CdTe compound is related as a solid solution with either stoichiometric CdTe as a solvent and excess pure Te atoms as solute, or congruently-grown CdTe (Te-rich) as the solvent and excess Cd or Te as the solutes. Although it is unknown that which the solvent physically exists, its data still can be treated. Judging from the experimental data, more accurate pressure reading is achieved when one component is dominant and the other is negligible (e.g. P_{Cd} reading is more accurate when $P_{Cd} \gg P_{Te2}$). For symmetrical reason, we choose point V as the solvent composition, which is close to congruent sublimation point C and the lowest total pressure point. The point Vs under four temperatures are deduced and fitted by equation

$$V(T) = [50 + \alpha \exp(\beta T)]100\% \qquad (10)$$

where the fitting parameter $\alpha = 2.511 \times 10^{-6}$ and $\beta = 0.005635$, as shown in Fig. 3. Using Eq. (10), we can estimate the point V at the growth temperature range (820–1000 K), adjacent to the experimental data. However, such fitted point V in Eq. (10) is only a reference close to the point where the two partial pressure curves cross.

The fitted curve using Eq. (9) as a function of solute molar number a (calculated from Eq. (6)) is shown in Fig. 4, where the Cd curve is fitted when Cd pressure is dominant and the Te curve is fitted when Te_2 pressure is dominant. The fitted curve is tolerable when the molar number a is between 0 and 1×10^{-4} under these four temperatures. The fitting parameters of Eq. (9) are then plotted as a function of temperature T, as shown in Fig. 5, where H_0 is fitted by Clausius–Clapeyron relation as a function of T and others are fitted linearly.

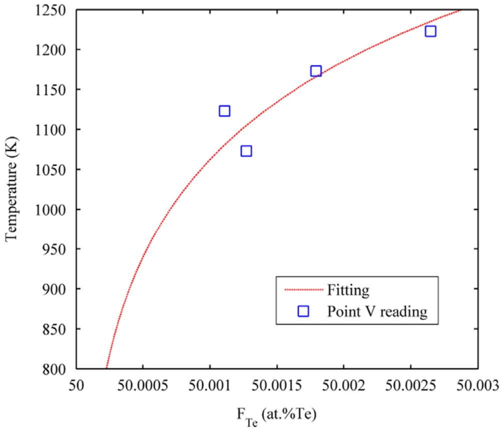

Fig. 3. The fitting of point V as a function of temperature T.

The growth model for diffusion-limited transport is discussed previously [1] and the equations under steady state

$$\begin{cases} J_{Cd} = \frac{D_{Cd}}{R\overline{T}h}[P_{Cd}(F_{sou}, T_{sou}) - P_{Cd}(F_{sub}, T_{sub})] \\ J_{Te} = \frac{D_{Te}}{R\overline{T}h}[P_{Te2}(F_{sou}, T_{sou}) - P_{Te2}(F_{sub}, T_{sub})] \\ J_{Cd} \approx 2J_{Te} \end{cases} \qquad (11)$$

yield one equation and two unknowns which is the source material composition F_{sou} and the substrate grown material composition F_{sub}. In Eq. (11), J_{Cd} and J_{Te} are the molar fluxes of Cd and Te_2 per unit area per unit time (mol m^{-2} s^{-1}) respectively, R is the ideal gas constant in unit of m^3 Pa K^{-1} mol^{-1}, $\overline{T}$ is the average temperature of the source and the substrate in unit of K, D_{Cd} and D_{Te} are the diffusivity coefficients of Cd and Te_2, respectively, in unit of m^2 s^{-1} and h is the spacing between the source and the substrate in unit of meter. When helium is used as the carrier gas, the system can be treated as a binary gas diffusion system of Cd/He or Te_2/He. The diffusivity coefficients of Cd and Te_2 atoms in the binary system are carefully derived in the

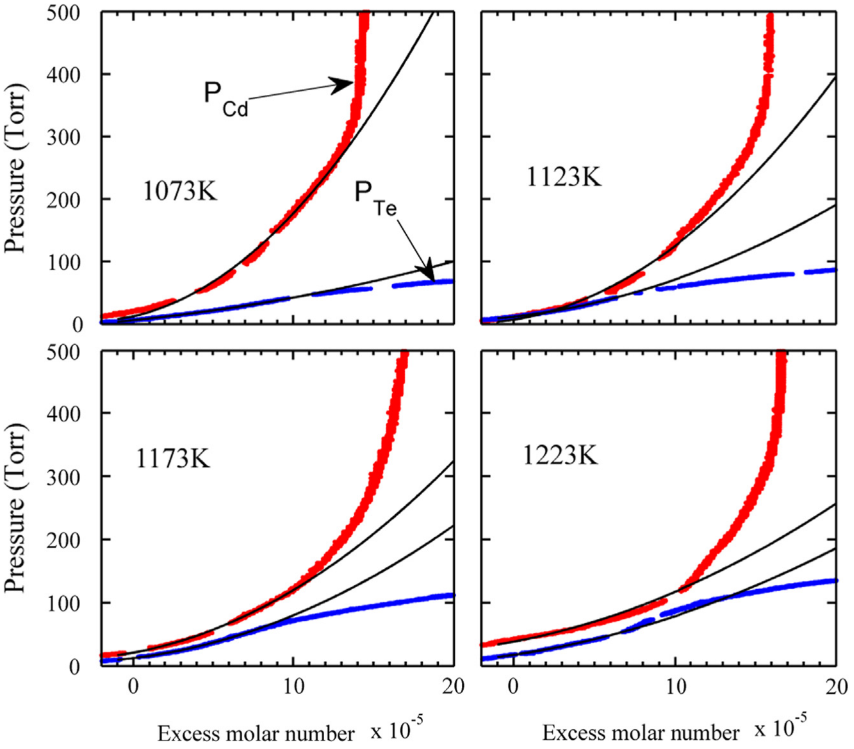

Fig. 4. Curve fittings of solute vapor pressure as a function of solute molar number in the solvent.

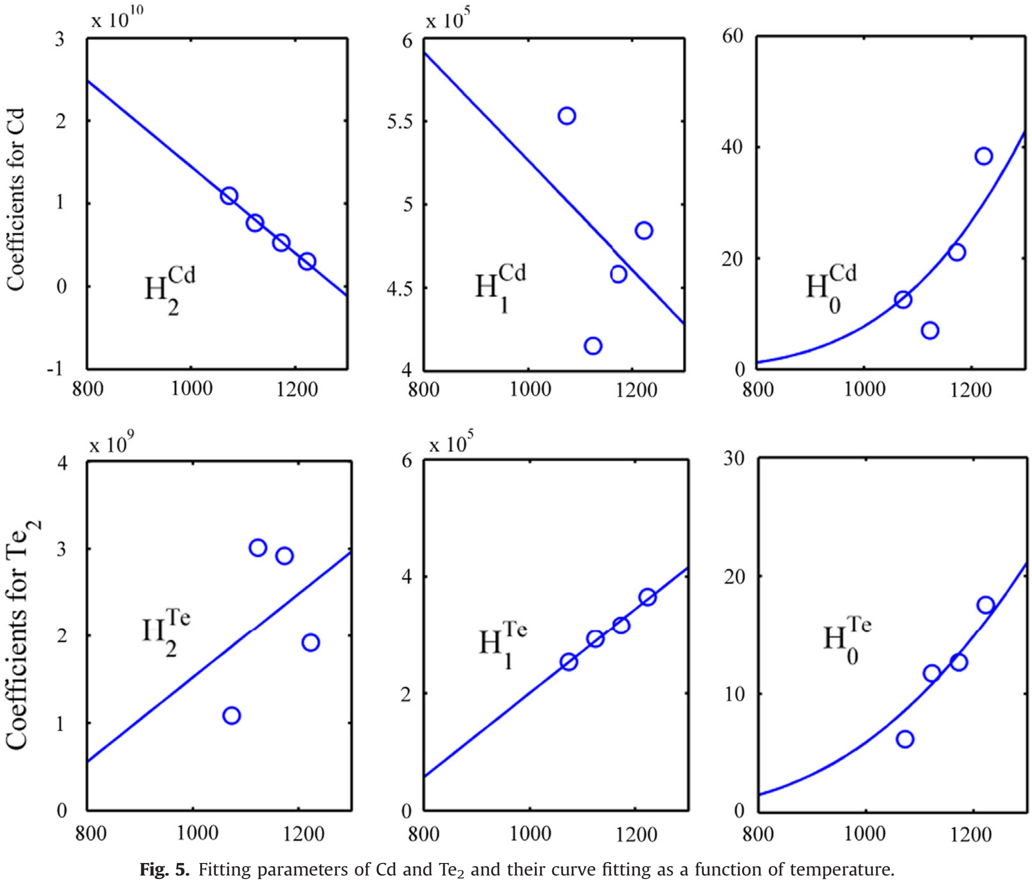

Fig. 5. Fitting parameters of Cd and Te_2 and their curve fitting as a function of temperature.

Stefan–Maxwell form [5]

$$D_{i,j}=\frac{3k\overline{T}}{8P_{total}\sigma_{i,j}^{2}}\left[\frac{k\overline{T}}{2\pi}\left(\frac{1}{m_i}+\frac{1}{m_j}\right)\right]^{1/2}, \tag{12}$$

where the calculated D is in unit of $\mathrm{m^2\,s^{-1}}$, k is the Boltzmann constant in unit of $\mathrm{J\,K^{-1}}$, $\sigma_{i,j}$ is the average collision diameter in unit of meter ($\sigma_{i,j}=½\sigma_i+½\sigma_j$), P_{Total} is the total pressure in unit of Pascal and m is the molecular (atomic) mass in unit of kilograms. The collision diameters as a function of temperature can be calculated using [1]

$$\sigma(T)=\sigma_{\infty}(1+C/T)^{1/2}, \tag{13}$$

with coefficients used by Bube et al. [1]. To get correct dimension and magnitude, all the units have been carefully treated. On the source side, the solute molar numbers of Cd and Te_2 can be calculated from F_{sou}. On both the source and the substrate, the partial pressure of the dominant component can be calculated by Eq. (9) using the fitted parameters as a function of temperature, while the partial pressure of the other component can be calculated by Eq. (8). Thus the solute molar numbers of the grown material under lower temperatures can be calculated and then its composition can be determined.

2.3. Model results

The source material composition F_{sou}, the source temperature ($T_{sou}=940$ K) and the substrate temperature ($T_{sub}=800$, 840 and 880 K) are assigned as input of Eq. (11). The background Helium pressure is 50 Torr and the distance between the source and the substrate is 4 mm. The calculated molar number shifts under different substrate temperatures are shown in Fig. 6, where the positive number indicates that the composition of the substrate material shifts towards more Te-rich compared to the source material. The molar number shift is equivalent to adding x moles of Te into 1 mol of the source material. Although the compositional shift is too small to measure, it may affect the crystal stoichiometry and significantly change the electrical property of the material. It is also shown that higher the temperature difference between the source and the substrate results in more composition shift.

The growth rate (μm/min) can be calculated from the material flux by

$$GR=\alpha\frac{J_{Cd}M_{CdTe}}{\rho_{CdTe}}60\times10^{6}, \tag{14}$$

where the coefficient α is sticking coefficient, M_{CdTe} is molar mass in kg/mol and ρ_{CdTe} is the density in $\mathrm{kg/m^3}$. The sticking coefficient is fitted to be 0.36 [2]. Physically, sticking coefficient means that only part of the evaporated materials will stay on the surface of the substrate. Sticking coefficient has a strong effect on material utilization efficiency. We think there are some other reasons that will result in the discrepancies between the calculations and the experimental results, such as temperature gradient from the thermocouple to the surface of the substrate and to that of the source, crucible edge material leakage, surface oxidation of the source material, voids in the grown film, transient of the system and so on. In this work, we tried to start the discussion without these complicated actual conditions and focus on the simple thermodynamic solutions, so the sticking coefficient will be ignored and a unity coefficient will be used. Fig. 7 shows the diffusivity coefficients of Cd and Te_2 as a function of source material composition. It is clear that the diffusivity which is inversely proportional to the total pressure limits the flux of material transport. The calculated growth rate is shown in Fig. 8, assuming α is unity. The maximum growth rate is achieved at the point V of that deposition temperature ($P_{Cd}=2P_{Te2}$). When P_{Cd} dominates, the growth rate is significantly limited. It is also suppressed gradually when P_{Te2} is dominant.

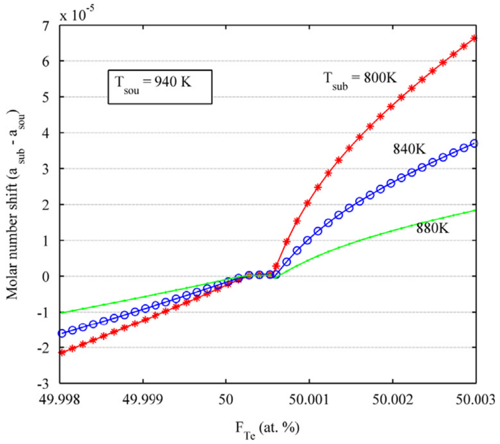

Fig. 6. The calculated grown material (substrate) molar number shift under three different substrate temperatures as a function of source material composition.

The calculation of deposition rate pales in front of the experimental result in many aspects. First of all, experimentally, the sticking coefficient α is undetectable. For small experimental setups, α may also include the undetectable losses of the source material from the edges or carried away by the ambient gas. Second, by decreasing the helium background pressure to <30 Torr, the calculated growth rate using diffusion model becomes unreasonably larger than the

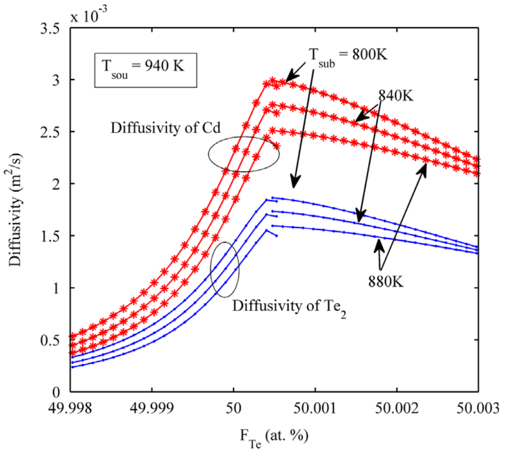

Fig. 7. Calculated diffusivity of Cd and Te_2 during CSS under different substrate temperature as a function of source material composition.

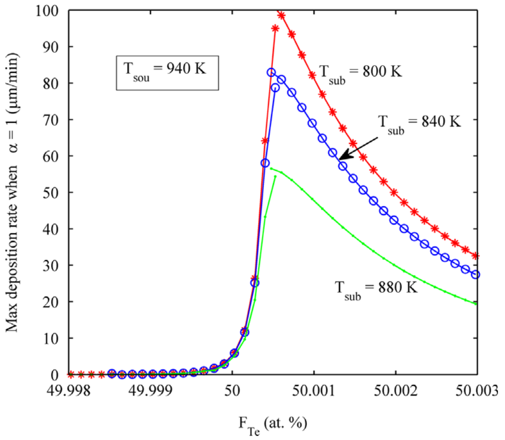

Fig. 8. Calculated growth rate as a function of source material composition under different substrate temperatures, assuming the sticking coefficient is unity.

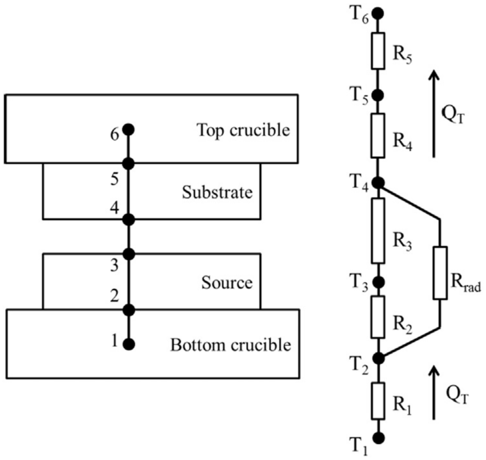

Fig. 9. The thermal analysis diagram of the CSS systems and equivalent heat circuit.

experimental result, because the deposition mechanism is changing from diffusion limited to sublimation limited [2]. Third, the design of the CSS crucible can limit the deposition rate. For bigger CSS systems, the actual temperature on the surface of the substrate, which is meant to be controlled by the substrate heater (top heater), may be affected by the radiation heating from the source. As shown in Fig. 9, the thermal analysis diagram shows the total heat flow Q_T from the bottom plate to top plate [1]. Ideally, there is a big thermal resistance (R_3 in Fig. 9) between the source and the substrate surfaces due to the physical gap between the source and substrate. In addition to heat transport by conduction and/or convection through the carrier gas (R_3), there is also a parallel radiative component from the source (shown as the extra path through R_{rad}). The radiation component limits the maximum of the temperature difference ΔT between T_4 and T_3, and thus limits the maximum deposition rate achievable for the system. Moreover, during dynamic fabrications with substrate transportation, there is an extra vacuum gap between the substrate and the top crucible surface, limiting the temperature difference ΔT between the source and the grown materials. In these cases, the actual deposition rate is not only affected by the sticking coefficient.

It must be pointed out that the system in the calculation is assumed to be in steady state with constant composition of the materials on the source and the substrate and with zero loss from edge leakage/oxidation. However, the system in reality is more complicated, resulting in more severe non-stoichiometric shift of grown material. First, in real CSS deposition crucibles, the source material is in the form of grains with limited mass. As predicted from Fig. 7, the composition of the source material will shift towards the composition at point *V*. Second, the oxygen induced into the system will consume Cd, making the source/substrate more Te-rich and increasing the deposition rate if the source material is initially stoichiometric. Third, materials will leak out from the edge of the crucible. Due to atomic mass difference, the diffusivity of Cd atoms is always bigger than that of Te_2 molecules, leading to severe non-stoichiometric loss of materials e.g. “Knudsen cell” model. In those cases, the stability of the CSS deposition can be affected in the long run.

At higher substrate temperatures, surface reactions will likely play a major role in growth. For example, at high substrate temperatures, neither Cd nor Te will stick unless they either react to form the less volatile CdTe phase. This is also why O_2 is sometimes added to the gas phase since oxides like CdO and TeO_x are less volatile than Cd or Te and provide an additional path to forming CdTe. The solubility of Cd or Te in CdTe also plays a role in the growth. For example, a Cadmium molecule can dissolve in the existing solid-phase CdTe on the substrate before reacting with Tellurium until it is saturated. If the solid-phase CdTe is already saturated with Cd or Te atoms, the Cd or Te cannot stick unless they either react to form the less volatile CdTe phase.

3. Conclusion

Based on the experimental data of partial pressures of CdTe vapor phases and diffusion transport equations, the grown substrate material compositions are calculated as a function of the source material composition and other growth conditions. The solid phase $Cd_{1-\delta}Te_{1+\delta}$ compound in the source material under CSS deposition temperature is treated as a solid solution with *a* mole of excess pure Te or Cd as solute and one mole of CdTe at composition point *V* as solvent, at which point the partial pressures of Cd and Te_2 are 1:2 (stoichiometric). Assuming the vapor pressures of Cd and Te_2 can be calculated using the law of solid solution $P_{Te2/Cd}=H_0+aH_1+a^2H_2$ round the composition point *V*, the experimental partial pressure curves under higher temperatures (1073–1223 K) as a function of solute molar number *a* are fitted. The coefficients H_i under the CSS temperatures are calculated from extensions of the existing experimental data under higher temperatures. As a result, by putting the calculated partial pressures into the diffusion transport equations, the molar number shift of the grown CdTe thin film and the growth rate, as functions of the molar number of the source material, are determined.

It is shown that the composition of the grown CdTe from a more Te-rich source material than the composition at point *V* will become more Te-rich. This shift may create more Cd vacancies and/or more Te interstitials. It is also shown that the composition of the grown CdTe from a more Cd-rich source material than the composition at point *V* will become more Cd-rich, which may decrease the Cd vacancies and/or increase Cd interstitials and Te vacancies. The composition at point *V* is almost the congruently-grown composition, which divides the two different composition shift directions. Additionally, larger temperature difference between the source and the substrate results in larger composition shifts. Lastly, the growth rate peaks at the composition point *V* and it becomes severely suppressed at more Cd-rich compositions.

From the calculated results, it is discussed that in principle the CSS technology itself is reliable, because stable deposition can be achieved at the congruent-growth composition which is close to composition point *V*. However, in reality the stability of the CSS deposition will be affected in the long run, for example, by limited amount of source material, poorly-controlled reaction oxygen concentration, non-stoichiometric edge leaking of source materials or limited surface reactions.

Acknowledgment

The authors acknowledge the China Triumph International Engineering Co. (CTIEC), Shanghai, China, which offers generous financial support for this work. They also thank Dr. Timothy Gessert and Dr. Jacob H. Greenberg for helpful discussions and technical support.

References

[1] T.C. Anthony, A.L. Fahrenbruch, R.H. Bube, Growth of CdTe films by close-spaced vapor transport, J. Vac. Sci. Technol. A 2 (1984) 1296.
[2] J.L. Cruz-Campa, D. Zubia, CdTe thin film growth model under CSS conditions, Sol. Energy Mater. Sol. Cells 93 (2009) 15–18.
[3] J. Ma, D. Kuciauskas, D. Albin, R. Bhattacharya, M. Reese, T. Barnes, J.V. Li, T. Gessert, S.-H. Wei, Dependence of the minority-carrier lifetime on the stoichiometry of CdTe using time-resolved photoluminescence and first-principles calculations, Phys. Rev. Lett. 111 (2013) 067402.
[4] J.H. Greenberg, *P–T–X* phase equilibrium and vapor pressure scanning of non-stoichiometry in CdTe, J. Cryst. Growth 161 (1996) 1.
[5] R. Eslamloueyan, M.H. Khademi, A neural network-based method for estimation of binary gas diffusivity, Chemom. Intell. Lab. Syst. 104 (2010) 195–204.